PERGAMON

International Journal of Heat and Mass Transfer 43 (2000) 643–652

International Journal of HEAT and MASS TRANSFER

www.elsevier.com/locate/ijhmt

Technical Note

Experimental results of the time to the onset of ice formation at metal surface and a correlation based on a sub-layer reactor model

Xiao Dong Chen*, Ping Chen, Kevin W. Free

Department of Chemical and Materials Engineering, The University of Auckland, Private Bag 92019, Auckland, New Zealand

Received 20 August 1998; received in revised form 20 April 1999

1. Introduction

Crystallization on heat exchanger surfaces is one of the major types of fouling and generally has three phases: induction, continuous growth and leveling off. It is difficult to find a satisfactory model to correlate the induction time. Ice forming onto heat exchanger surfaces is common in food industry, as many processes require low temperatures, e.g. the making of ice beer, ice cream, chilling of fruit juices, freeze concentration, storage of raw milk, etc. Short induction time is preferred in the cases where ice is also a part of the product. Many studies of industrial nucleation and crystallization kinetics have focused on the behavior of suspension crystallizer and the flow parameters are not precisely and explicitly incorporated. For example, measuring nucleation rate using differential scanning calorimetry (DSC) for small amount of liquid with large super-cooling (about 10°C) [1] and a recent study carried out at Unilever [2] which assumes that the nucleation rate is proportional to the super-cooling temperature to some power. The most related study to the current work was that by Arora and Howell [3] in 1973, where they investigated freezing of super-cooled brine in forced turbulent flow inside circular tubes. However, their model is less rigorous in assuming nucleation to occur at a specific temperature as opposed to applying a nucleation rate. The super-cooling was varied within 4°C. In this study, experimental data on the time to the onset of ice formation have been obtained. In the present study we observed the onset of ice formation inside a copper tube placed after a cooling coil. We are interested in the 'induction time' of the process under carefully controlled fluid flow conditions. Pure water and sucrose solutions were used. A mathematical model based on the sub-layer reactor model, originated from the reaction fouling study by Paterson and Fryer [4], has been adapted to correlate the induction time (t_i) for this particular process.

2. Experimental

2.1. The apparatus and the testing fluids

The apparatus for determining the onset of crystallization (i.e., ice formation in this case) from flowing aqueous solution is shown in Fig. 1a. The main components are two separate flow loops, one for the coolant flow and the other for the aqueous solution, and the data acquisition system. The cooling system incorporated a heat reservoir in which, the temperature of the coolant could be kept constant. Glycol solution 50 wt%, in a 20 l tank (8) was used as the coolant and was chilled by a 2 kW freezer (10) (also refer to Fig. 1). The temperature of the glycol was measured using a PT100 probe and it was controlled within ±0.5°C by an ASCON PID controller (6). The glycol solution

* Corresponding author. Tel.: +64-9-3737599-x-7004; fax: +64-9-3737463.

E-mail address: d.chen@auckland.ac.nz (X.D. Chen)

PII: S0017-9310(99)00145-3

Nomenclature

A	modified reaction frequency factor, s^{-1} (see Eq. (9))
A_0	apparent reaction frequency factor, s^{-1} (see Eq. (1))
B	a variable defined in Eq. (8)
C	a variable defined in Eq. (11)
c_s	solute concentration, kg m^{-3} (see Eq. (18))
d	tube inner diameter, m
E	apparent activation energy, J mol^{-1} (see Eq. (1))
j	power of the dependence function of E upon super-cooling temperature (ΔT)
m	reaction order in Eq. (1)
N	number of nuclei in the laminar sub-layer, m^{-2}
n	nuclei concentration, m^{-3}
T	temperature, K
t	time, s
t_i	induction time, s
ΔT	super-cooling temperature, °C
U_∞	bulk fluid velocity, m s^{-1}
U^*	friction velocity, m s^{-1}
δ	laminar sub-layer thickness, m
ρ	fluid density, kg m^{-3}
ν	kinematic viscosity, m^2 s^{-1}
τ_0	shear stress, N m^{-2}

Subscripts

ave	average
b	bulk
bath	cooling bath
c	critical
FP	freezing point
g	glycol solution
H	high
in	inlet
out	outlet
s	solution or solute
w	wall
∞	bulk

was circulated between the 6 l Grant Barrington low temperature bath (3) and the glycol tank (8) by a DP K3/4 circulating pump (7). The temperature in the cooling bath (3) which was adjusted by an immersed circulating heater (5) could be set to desired temperatures with fluctuations within ± 0.2°C. The glycol solution level in the cooling bath (3) was kept constant by an overflow mechanism. The fluids tested were distilled water, 10, 20 and 31 wt% sucrose solutions. In each run, the test fluid was pre-cooled to about 0°C in a domestic refrigerator and then filled into the 10 l insulated solution tank (1). A copper coil (4) (8 mm outer-diameter and 0.8 mm wall thickness) was used as the test section. The copper coil was held by a Perspex plate at the upper end to position the coil in the coolant. The fluid was pumped through the copper coil (4) by a RS magnetic coupled pump (Ratio Spares Components, UK) (2). Solution flow was adjusted using the speed controller of this pump (2). The whole system was insulated wherever appropriate. Thermocouples for measuring the wall temperatures of the coil and the inlet and outlet temperatures of the solution flow were made of OMEGA teflon insulated (Φ 0.07 mm) type T thermocouple wires. The locations of the wall temperature and fluid temperature thermocouples are shown in Fig. 1b. The inlet and outlet flow temperatures were measured by two calibrated thermocouples threaded through two Φ 0.8 mm syringe needles. The welded point of each thermocouple was located at the needle top. The thermocouple needles were then put through pre-drilled holes in the wall of the cooling coil and the needle tips were placed at the tube center and then welded onto the coil wall (see Fig. 1b). For the wall temperatures, four thermocouples were glued into blind holes cut into the outer surface of the cooling coil. The measuring points were set on the vertical section of the coil, which was close to the outlet and just below the cooling liquid level, to determine the position of the onset of crystallization. There was a 2 cm distance between any two neighboring points. It has been found that the temperature difference between the neighboring two points were within ± 0.2°C when ice started to form on the inner wall. The voltage signals from the thermocouples were converted to digital signals by KEITHLEY data acquisition boards and recorded by an IBM 486 computer. The flow rates of two flow loops were also measured using the RS flow sensor. It was important to detect if there was any secondary flow (due to the coiling) influences upon the temperature measurements at the locations shown in Fig. 1b (i.e., Those at T_1 and T_2), and the possible influence on the sub-layer formation. To achieve this, a plastic coil of similar size, (inside diameter of 6 mm, shown in Fig. 2 where the flow went from laminar regime through transitional regime to turbulence regime) was made to allow visualization to be carried out for pure water. It has been shown that there was no visible secondary flow beyond the point of 3 cm below T_2 measurement. In our experiments on ice formation, sample fluids used were of higher viscosities; thus the conclusions drawn from this visualization work would still be valid. Secondary flow due

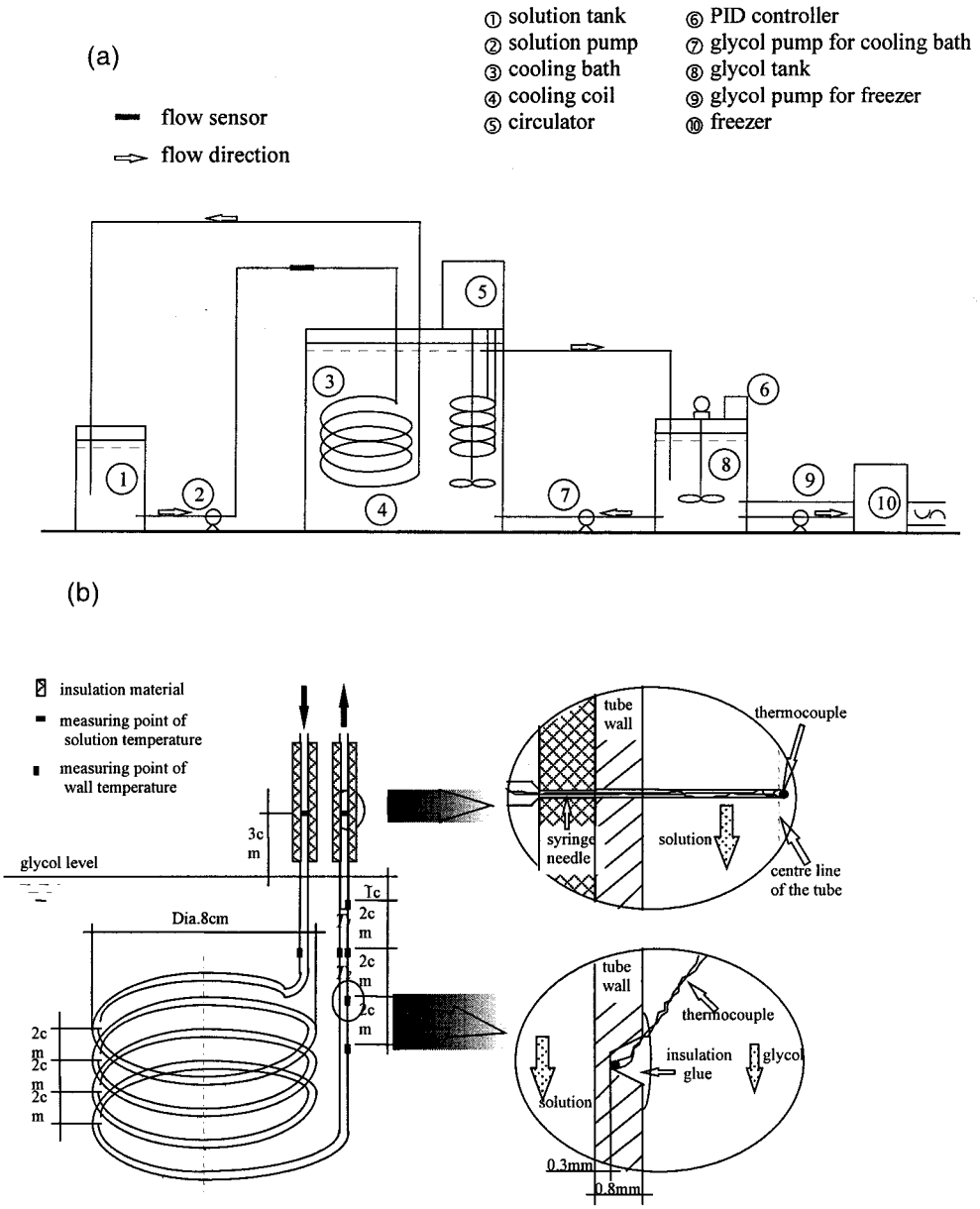

Fig. 1. Schematic diagram of the experimental apparatus.

to coiling disappears in the region 3 cm before the T_2 measuring point and would not affect the results presented in this paper.

2.2. The induction time (t_i) measurement

Typical curves recorded for each experimental run are shown in Fig. 3 for 10 wt% sucrose solution. The curves of fluid velocity in the coil (U_∞), cooling bath temperature (T_{bath}), inlet and outlet temperatures of the fluid (T_{in} and T_{out}) and the wall temperatures of the two nearest points to initial ice formation (T_1 and T_2) are all plotted in this diagram. Note that, in general, the inlet and outlet temperatures decrease only slightly during each experiment until ice started to form. The induction time is defined as 'the time from the point where the outlet temperature reaches the

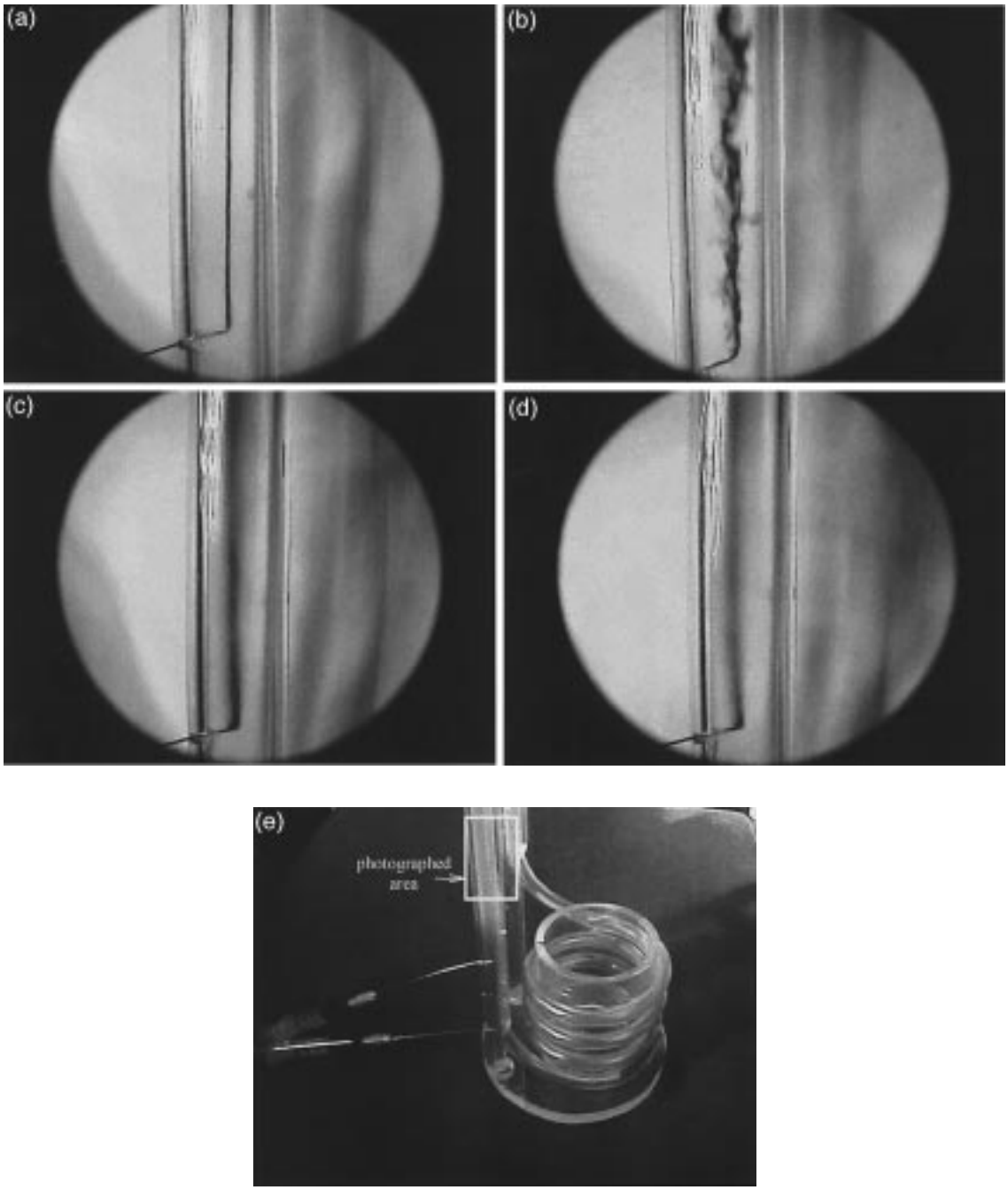

Fig. 2. Flow visualization of the test section (a–d: different velocities; e: the set-up of the test section).

freezing point temperature for the test solution to the point beyond which crystallization occurs, i.e., the point A on the diagram'. Around point A, the outlet temperature starts to rise and the flow velocity begins to decrease. One can see that each experiment may be divided into four stages:

Stage I: The fluid is cooled by the glycol flow around the coil when the coil is dipped in the cooling bath. The wall temperatures decrease rapidly during this stage

Stage II: The fluid temperatures decrease gradually. The solution flows in the coil with a certain amount

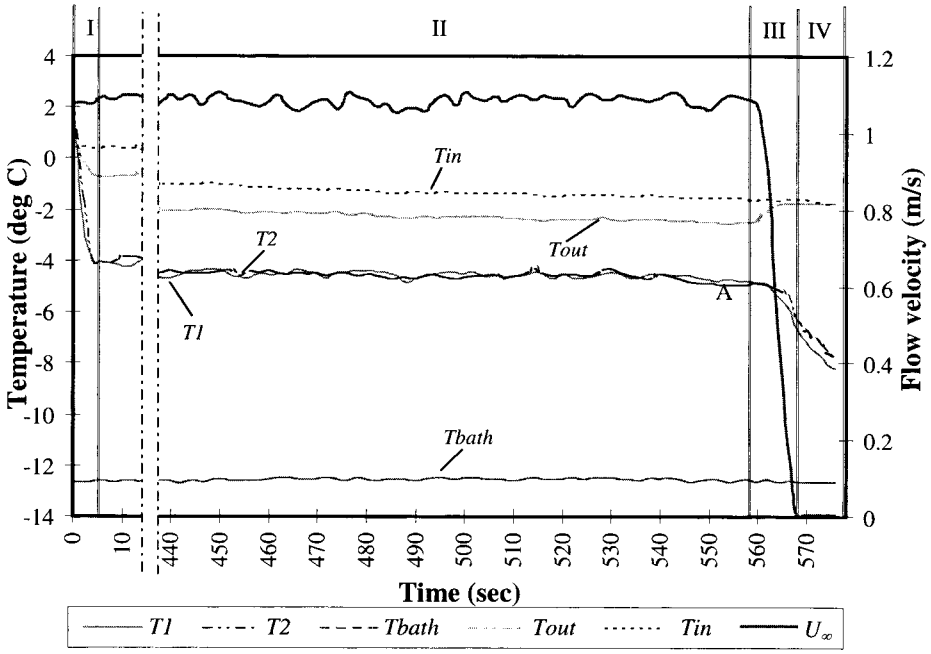

Fig. 3. Typical measuring curves for 10 wt% sucrose solution (where point A is the terminal point of t_i measurement).

of sub-cooling that is not yet sufficient to enable a continuous crystallization

Stage III: The nucleate size or population near the tube wall becomes larger than the critical size and starts to grow at a finite rate. The outlet temperature of the solution starts to rise. In many cases, we could observe numerous small 'crystals' starting to gush out of the coil into the solution tank and this could also be taken as an evidence of the start of 'auto' ice formation

Stage IV: The ice blocks the cross-section of the tube and starts to grow along the tube. The wall temperatures reduce dramatically.

The start of ice formation on the inner wall of the copper tube was taken as the transition between Stages II and III (i.e., around point A within ± 25 s). In this work, the onset temperatures (the temperatures taken at point A in different runs) and the induction times for distilled water and sucrose solutions (i.e., 10, 20 and 31 wt%), were measured. These were done under various conditions such as the cooling bath temperatures (about -15.55 to -5.5°C), the flow velocities (0.15–1.9 m s^{-1}). The freezing points of all the solutions used here were those measured by the same authors [5]. The Reynolds number was varied below or above the critical Reynolds number, for smooth pipe flow (i.e., $Re_c \approx 2300$): for water trials Re = 537–3766; for 10 wt% sucrose solution Re = 517–3594; for 20 wt% sucrose solution Re = 948–3436 and for 31 wt% sucrose solution Re = 529–1977, respectively.

3. The development of a sub-layer reactor model for the onset of ice formation

3.1. The basic nucleation rate equation

According to nucleation and crystallization theories described previously [6–8], the condition under which liquid starts to nucleate is determined by the free energy change when the material changes from liquid to solid state. Combining the existing knowledge of nucleation, as recently described by Bansal et al. [9], we can expect that the nucleation rate in a batch fluid may be expressed in the form of the Arrhenius rate equation:

$$\frac{dn}{dt} = A_0 e^{-\frac{E}{RT}} (n)^m \quad (m^{-3}\ s^{-1}), \tag{1}$$

where n is the nuclei concentration in the fluid near metal surface (m^{-3}); T is the temperature (K); E is the apparent activation energy of the process (J mol^{-1}); A_0 is the apparent frequency factor (s^{-1}); R is the univer-

sal gas constant (= 8.31 J mol^{-1} K^{-1}). Eq. (1) can be seen as an attempt to address the following two key issues: (a) nucleation (a heterogeneous process involving metal surface) is an activation process, i.e., $E > 0$; (b) the nuclei concentration dependence (with m, the order of 'the chemical reaction process'), which allows for the mechanism, whereby, the more nuclei generated the greater possibility for more to generate.

3.2. The 'sub-layer' reactor model (flow condition)

The concept of 'sub-layer reactor' was adopted from milk fouling research carried out by Paterson and Fryer [4], Fryer et al. [10] and Belmar-Beiny et al. [11]. We have found this model useful in our own recent fouling work on concentrated milks (not yet published) which is related to the present study. Another model for the initial chemical reaction fouling is the one proposed by Epstein [12], which correlates extremely well for hydrocarbon fouling. In the present case, we assume that the nuclei concentration in the bulk is negligible, so the activity associated with ice forming at the metal surface is confined within the sub-layer. Also, the survival of the nuclei generated at near wall region is controlled by the temperature gradient (thus controlled by sub-layer thickness). This view is more closely related to milk fouling [1]. When the wall temperature becomes lower than the freezing point of the solution, nuclei are expected to generate in the near wall region. The driving force for the generation of nuclei is the super-cooling temperature at the wall ($T_w - T_{FP}$, where T_{FP} is the freezing temperature). We assume that the nucleate concentration (or the effectiveness of the nuclei for triggering crystallization) decreases rapidly, approaching the laminar sub-layer thickness or a thickness that is proportional to the sub-layer thickness. The extent of nucleation, leading to crystallization, depends on the size of the reactor, i.e., the laminar sub-layer thickness (δ) or a fluid 'layer' proportional to the sub-layer thickness. When the flow becomes laminar, according to the text book value of Reynolds number, the extrapolated thickness may still be useful at least as a scaling factor. We assume that a critical concentration (n_c) exists at the near wall region (inside the sub-layer) for each flow or thermal condition. Crystallization (ice formation) occurs rapidly as soon as n_c is attained. The time taken to reach n_c is taken to be the experimental t_i. Based on this argument, the rate of nucleate generation within the sub-layer reactor is the determining factor for t_i. This rate may be expressed in terms of per unit area of the sub-layer (or expressed to be proportional to the sub-layer if only using the sub-layer thickness as a scaling parameter rather than its exact value, but this will not change the outcome of this work), i.e.,

$$\frac{dN}{dt} = \delta \frac{dn_{ave}}{dt} = A_0 \delta^{1-m} e^{-\frac{E}{RT_{ave}}} N^m \tag{2}$$

where, N is the number of the nuclei within the sub-layer ($= n_{ave}\delta$) per unit surface area (m^{-2}); n_{ave} is the average nuclei concentration in the sub-layer; T_{ave} is the average temperature in the sub-layer (taken to be $\approx (T_w + T_{FP})/2$). The thickness of the sub-layer may be obtained according to the boundary layer theory for internal turbulent flow. From the universal velocity-distribution law for a smooth pipe [13], the following relationship for determining the laminar sub-layer thickness is used:

$$\log\left(\frac{\delta U^*}{\nu}\right) = 1 \quad \text{or} \quad \delta = 10\frac{\nu}{U^*} \tag{3}$$

where ν is the kinematic viscosity (m^2 s^{-1}) and U^* is the friction velocity (m s^{-1}). The shearing stress at the wall is also given by Schlichting [13] as below:

$$\tau_0 = \rho (U^*)^2 \approx 0.03955 \rho U_\infty^{\frac{7}{4}} \nu^{\frac{1}{4}} d^{-\frac{1}{4}}, \tag{4}$$

where ρ is the fluid density (kg m^{-3}) and d is the pipe inner diameter (m). Substituting Eq. (4) into Eq. (3), we obtain:

$$\delta = 50.3\left(\frac{\nu}{U_\infty}\right)^{\frac{7}{8}} d^{\frac{1}{8}} \tag{5}$$

Eq. (2) can then be re-written after substituting δ in (2) with (5):

$$\frac{dN}{dt} = \left(50.3 d^{\frac{1}{8}}\right)^{1-m} A_0 e^{-\frac{E}{RT_{ave}}} \left(\frac{\nu}{U_\infty}\right)^{\frac{7}{8}(1-m)} N^m \tag{6}$$

t_i is expressed by integrating (6) from $t = 0$ (when $T_b \approx T_{FP}$) to t_i (when $T_w \approx T_{onset}$):

$$t_i = \left(\frac{U_\infty}{\nu}\right)^{\frac{7}{8}(1-m)} \frac{1}{A e^{-\frac{E}{RT_{ave}}}} \int_{N_0}^{N_c} \frac{1}{N^m} dN$$

$$= \left(\frac{U_\infty}{\nu}\right)^{\frac{7}{8}(1-m)} \frac{B}{A e^{-\frac{E}{RT_{ave}}}} \tag{7}$$

where B is a constant at the onset of ice formation, i.e.,

$$B = \frac{N_c^{1-m} - N_0^{1-m}}{1-m} \tag{8}$$

and A is defined as

$$A = \left(50.3 d^{\frac{1}{8}}\right)^{1-m} A_0 \tag{9}$$

Note that when $t < t_i$, T_{ave} does not change much. In Eq. (7), N_c may be understood as the 'critical number' of the nuclei that has already reached critical 'size' for crystallization. We have also assumed here a non-zero initial value, N_0, to avoid singularity. This is reasonable as under the experimental conditions in this study, crystallization was inevitable (so N_0 should at least be 1 to start with). So far, we have outlined the approach employed in this study. The critical value (N_c) is the limiting condition of nucleation, which can not be measured directly. However, based on the fact that nucleation is a time-dependent process, t_i reflects N_c to a large extent. It should be interesting to note that we may replace the number concentration (n) with the so-called nucleate radius [6] but this would not affect the outcome of this study.

4. Application of the sub-layer reactor model in correlating the experimental induction time (the time to the onset of ice formation)

4.1. The apparent activation energy

For the same fluid velocity, Eq. (7) can be re-written as:

$$\ln t_i = C + \frac{E}{RT_{ave}} - \frac{7}{8}(1-m)\ln v, \tag{10}$$

where

$$C = \ln\left(\frac{B}{A}\right) + \frac{7}{8}(1-m)\ln U_\infty \tag{11}$$

It is not known if B/A depends on concentration or supercooling temperature. However, because $B \propto (N_c^m - -N_0^m)$ and N_c is proportional to surface tension (which normally reduces as solute concentration increases), freezing point temperature (which decreases as solute concentration increases) and the inverse of super-cooling temperature (ΔT) (which is greater for higher concentration), B should decrease with increasing concentration. A should also reduce as solute concentration increases partially due to less opportunity for water molecules to interact with existing nuclei with the strong presence of the solute molecules. A should also become smaller as super-cooling gets larger. Since, B and A both reduce as solute concentration reduces, there is a possibility that $B/A \approx$ constant, for the same fluid velocity. If true, C would be constant when the fluid velocity is kept constant. Given a value for m and for any two sets of t_i data obtained under the same solution velocity, using Eq. (10), we have

$$\ln t_{i1} = C + \frac{E}{RT_{ave,1}} - \frac{7}{8}(1-m)\ln \nu_1 \tag{12}$$

and

$$\ln t_{i2} = C + \frac{E}{RT_{ave,2}} - \frac{7}{8}(1-m)\ln \nu_2 \tag{13}$$

We can find E from two points, 1 and 2, from Eqs. (12) and (13):

$$E_{1-2} = \frac{RT_{ave,1}T_{ave,2}}{T_{ave,1} - T_{ave,2}} \ln\left[\frac{t_{i_1}}{t_{i_2}}\left(\frac{\nu_2}{\nu_1}\right)^{\frac{7}{8}(1-m)}\right] \tag{14}$$

To find the best value of m for the process, a progressive regression procedure was employed for m values varying from 0 to 3. The relationship of E vs. ΔT is assumed to be a power function, i.e., $E \sim \Delta T^{-j}$, according to the classic approach [6] where the power j was varied from 0 to 2.5 during data analysis (note that for homogeneous nucleation, $j = 2$). It was found that all the data from the distilled water and 10 wt% sucrose solution trials can be correlated regardless the flow regimes indicated by the Reynolds number. This means that at least the sub-layer thickness can be used as a scaling parameter for the boundary layer reactor size for the range of flows considered. The calculations for the fluids used in this study show that the 'sub-layer' reactor size as extrapolated from Eq. (5) is about 1 mm for laminar flow which is still small comparing with the inside diameter of the copper tube used. The viscosity and density parameters for water and sucrose solutions were taken from literature [14,15]. For the data collected, the best fit for j was found to be 1.67 and $m = 1.5$. The j value of 1.67 (not 2) reflects the nature of heterogeneous nucleation. This gives a correlation coefficient $r^2 = 0.824$ for activation energy against supercooling temperature (see Fig. 4a). E can now be expressed as a function of super-cooling temperature shown in Fig. 4 as the solid line of best fit using the expression:

$$E \approx 1076.85 \times 10^3 \Delta T^{-1.67} \tag{15}$$

4.2. The ratio (B/A)

The (B/A) can be calculated using Eqs. (7) and (15) using the experimental data and the related physical properties:

$$\frac{B}{A} = t_i\left(\frac{\nu}{U_\infty}\right)^{\frac{7}{8}(1-m)} e^{-\frac{E}{RT_{ave}}} \tag{16}$$

The calculated (B/A) values are plotted in Fig. 4b as a function of U_∞. It can be seen there, that the (B/A)

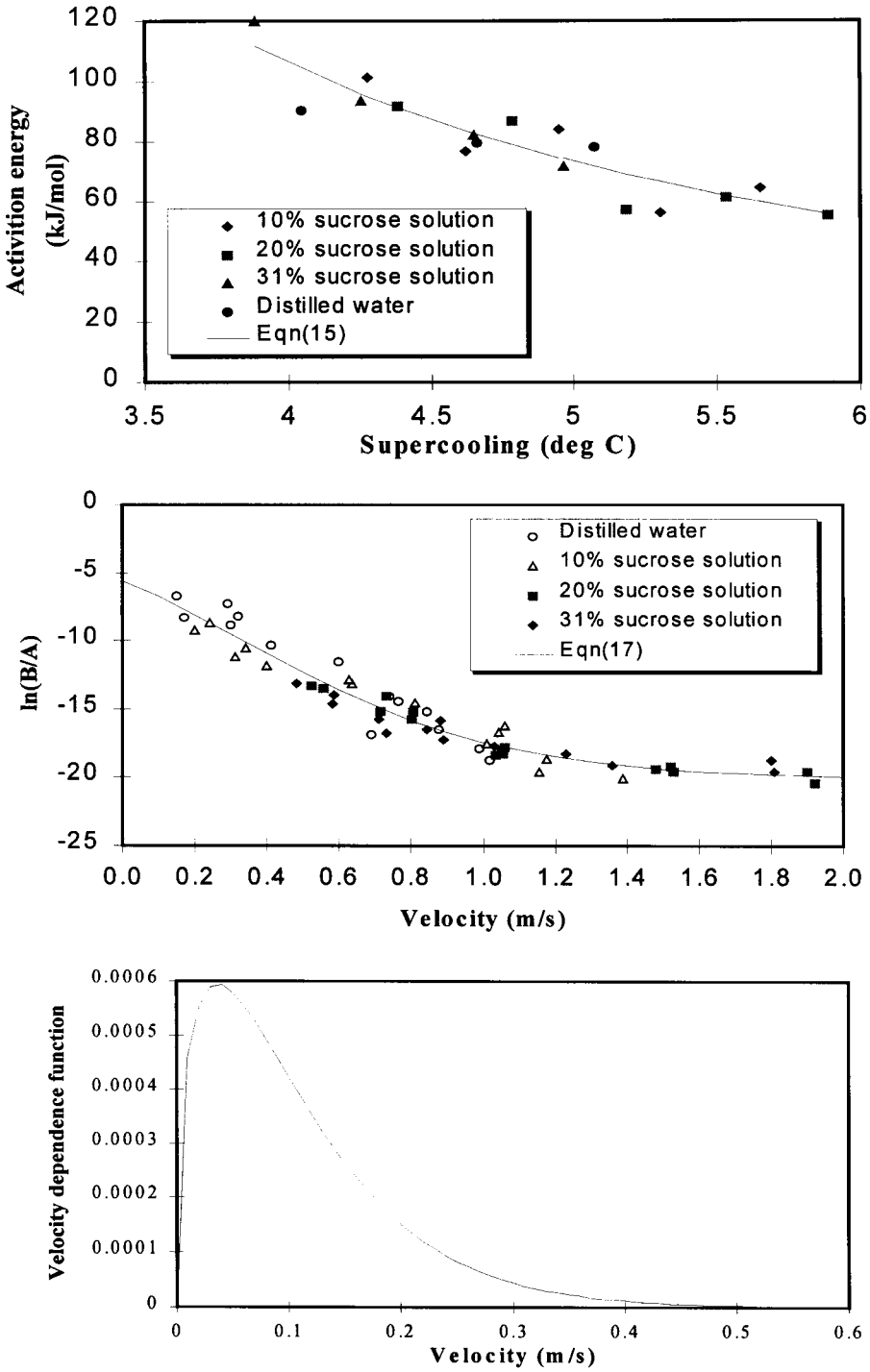

Fig. 4. Various dependence functions of the sub-layer reactor approach.

values for distilled water, tap water and 10, 20 and 31 wt% sucrose solutions fall on the same line which has been fitted as an equation (with $r^2 = 0.935$), which does not seem to be temperature dependent:

$$\frac{B}{A} = \exp\left(\frac{-20.1242}{1+\exp\left((0.3405-U_\infty)/0.3532\right)}\right) \tag{17}$$

4.3. Remarks

To summarize, the 'chemical reaction rate' equation for nucleation under flow conditions, i.e., Eq. (2), can be expressed in the form of the following, according to the analysis given above:

$$\frac{\mathrm{d}N}{\mathrm{d}t} = \left(50.3d^{\frac{1}{8}}\right)^{(1-m)} A_0 \mathrm{e}^{-\frac{E(\Delta T)}{RT_{\mathrm{ave}}}} \left(\frac{\nu(c_\mathrm{s},T_{\mathrm{ave}})}{U_\infty}\right)^{\frac{7}{8}(1-m)} N^m, \tag{18}$$

where c_s is the solute concentration (kg m^{-3}). The number of nuclei in the laminar sub-layer plays an important role in the nucleation rate, i.e., a reaction order $m = 1.5$ has been found to be appropriate, which is consistent with the work by Bansal et al. [9]. Under the current experimental conditions, the induction time can be expressed as below

$$t_\mathrm{i} = \left(\frac{\nu}{U_\infty}\right)^{\frac{7}{16}} \mathrm{e}^{\frac{-1076.85\times10^3\Delta T^{-1.67}}{RT_{\mathrm{ave}}} - \frac{20.1242}{1+\exp\left(\frac{0.3405-U_\infty}{0.3532}\right)}} \tag{19}$$

The effect of solution velocity can be shown by plotting the velocity dependence function $U_\infty^{7/8}(B/A)$ in Eq. (19) (see Fig. 4c). One can see that initially increasing velocity reduces the sub-layer thickness thus increasing the degree of difficulty of crystallization (thus greater t_i), but this effect is later overshadowed by another effect that gradually reduces t_i. The later is not yet fully understood and needs further study. It is interesting to note that although the sub-layer reactor concept assumes turbulence, for Reynolds numbers down to ~ 520, the data can also be well correlated using the above formula. This means that the sub-layer thickness may be taken to be proportional to the boundary layer reactor size even at low fluid velocities.

5. Conclusions

In this paper, experimental results of the time to the onset of crystallization for sucrose solutions of various concentrations are reported. A 'sub-layer reactor' model previously developed in reaction fouling studies has been extended to account for the induction process in ice formation from flowing aqueous solutions. The model adequately correlates the time to the onset of ice formation or the induction time for crystallization (t_i). The model may also be applied to more general crystallization fouling studies. Future experiments on the induction of crystallization fouling may be operated similarly in measuring the time taken before the first crystal or the first patch of crystals is formed on heat exchanger surface.

Acknowledgements

This work was supported by the New Zealand Dairy Board and the Electricity Co-operation of New Zealand.

References

[1] S. Charoenrein, D.S. Reid, The use of DSC to study the kinetics of heterogenous nucleation of ice in aqueous systems, Thermochimica Acta 156 (1989) 373–381.
[2] D.R.G. Cox, L.O. Heeney, S.R. Moore, M.E. Blades, Primary nucleation of ice from sucrose solutions, in: R. Jowitt (Ed.), Engineering and Food at ICEF 7, Sheffield Academic Press, Sheffield, 1997, pp. A224–A227.
[3] A.P.S. Arora, J.R. Howell, An investigation of the freezing of supercooled liquid in forced turbulent flow inside circular tubes, Int. J. Heat and Mass Transfer 16 (1973) 2077–2085.
[4] W.R. Paterson, P.J. Fryer, A reaction engineering approach to the analysis of fouling, Chemical Engineering Science 43 (7) (1988) 1714–1717.
[5] P. Chen, X.D. Chen, K.W. Free, Measurement and data interpretation of the freezing point depression of milks, J. Food Engng 30 (1996) 239–253.
[6] J.W. Mullin, in: Crystallisation, CRC Press, Butterworth, New York, 1972, pp. 136–232.
[7] G.X. Hu, M.G. Qian, in: Metallography, Shanghai Science and Technology Press, China, 1980, pp. 124–135.
[8] H. Schubert, A. Mersmann, Determination of heterogeneous nucleation rates, Trans. IChemE 74A (1996) 821–827.
[9] B. Bansal, H. Muller-Steinhagen, X.D. Chen, Effect of suspended particles on crystallisation fouling in plate heat exchangers, ASME J. Heat Transfer 119 (3) (1997) 568–574.
[10] P.J. Fryer, S.M. Gotham, W.R. Paterson, N.K.H. Slater, A systematic approach to the study and modelling of food fouling, in: Engineering Innovation in the Food Industry, Inst. Chem. Engrs, UK, 1989, pp. 111–129.
[11] M.T. Belmar-Beiny, S.M. Gotham, W.R. Paterson, P.J. Fryer, A.M. Pritchard, The effect of Reynolds number

and fluid temperature in whey protein fouling, J. Food Engng 19 (1993) 119–139.

[12] N. Epstein, A model of the initial chemical reaction fouling rate for flow within a heated tube, and its verification, in: Proceedings of 10th Int. Conf. Heat Transfer, Inst. Chem. Engrs, Brighton, 1994, pp. 225–229.

[13] H. Schlichting, in: Boundary-Layer Theory, 7th ed., McGraw-Hill, New York, 1979 (J. Kestin, Trans.).

[14] R.A. Keppeler, J.R. Boose, Thermal properties of frozen sucrose solution, Transactions of ASAE 13 (1970) 335–339.

[15] E.P. Liley, R.C. Reid, E. Buck, Physical and Chemical Data, in: R.H. Perry, D.W. Green (Eds.), 'Perry's Chemical Engineering Handbook, 60th ed., McGraw-Hill, Singapore, 1984, pp. 3–254.